RM-240

RESEARCH ON MOLECULE-SURFACE INTERACTION - PART II EXPERIMENTS ON THE FORMATION OF A SHOCK TUBE DRIVEN MOLECULAR BEAM

September 1964

Grumman
RESEARCH DEPARTMENT

GRUMMAN AIRCRAFT ENGINEERING CORPORATION
BETHPAGE NEW YORK

Grumman Research Department Memorandum RM-240

RESEARCH ON MOLECULE-SURFACE INTERACTION

PART II

EXPERIMENTS ON THE FORMATION OF A SHOCK TUBE DRIVEN MOLECULAR BEAM

by

Richard A. Oman and Vincent S. Calia
Fluid Mechanics Section

September 1964

Supported by the National Aeronautics and Space Administration
Physics of Fluids Program
Contract NASw-709

Approved by: Charles E. Mack, Jr.
Charles E. Mack, Jr.
Director of Research

FOREWORD

This Memorandum comprises the second part of a three-part final report on NASA contract number NASw-709. It describes one part of the experimental work performed under that contract, which is a successor to NASr-104 on the same subject, namely, the interaction of high energy gas particles with solid surfaces.

This research was performed under the technical supervision of the NASA Physics of Fluids Office, Mr. Alfred P. Gessow, Chief. It covers the period from July 1, 1963 to August 9, 1964.

Research Dept.
RM - 240
September 1964

ABSTRACT

33283

Experiments on several problems involved in the formation of a shock tube driven molecular beam are described. Particular attention is devoted to unsteady (starting) effects on skimmers and to measurements of stagnation heat transfer in the flow field upstream of the skimmer. The results of these experiments indicate a good configuration for operation with an impulsive source.

Author

Research Dept.
RM - 240
September 1964

TABLE OF CONTENTS

LIST OF ILLUSTRATIONS

INTRODUCTION

This Memorandum, Part II of a final report series on NASw-709, describes research conducted on a shock-tube-driven molecular beam. The device is being developed for experiments in molecule-surface interaction in the energy range from 0.1 to 10 EV per particle. Complementary parts of the over-all program are described in Part I, which deals with a theoretical analysis of molecule-surface interaction, and in Part III, which describes experiments on surface contamination, preparation, and analysis.

The test apparatus is discussed in Refs. 1 and 2, and only a brief description is given here. The goal of the present work is to determine the best means of forming a high intensity molecular beam for surface interaction work. Most of the discussion deals with problems encountered in getting a molecular beam through a skimmer efficiently. As with any experimental apparatus, many of the difficulties that have been encountered are unique to the particular design. However, there are several general phenomena that affect all high intensity molecular beams to some degree, and we feel some of our measurements and analyses will be quite helpful to other investigators using different approaches.

GENERAL DISCUSSION

There are several features of our apparatus that greatly affect the correct interpretation of the results which follow. These features are somewhat different from those found in steady-flow molecular beams with nozzle sources. The most obvious difference is the short time duration of the shock tube run, which provides the ability to maintain extremely low background pressures in the beam-forming regions. A less favorable effect is the unsteadiness produced by shock tube boundary layer interactions, which at low stagnation densities can make accurate determination of the true upstream conditions a difficult problem. It must also be remembered that we employ much higher levels of stagnation enthalpy and density than are normally the case in molecular beams; this results in correspondingly high expansion ratios to produce the pre-skimmer flow field. Our configuration ensures a very high Mach number at the skimmer, a situation that is not always the case at lower densities. The problem of predicting final Mach number is treated theoretically by Brook and Oman (Ref. 3) and was also discussed in Ref. 1. Recent measurements of molecular velocity distributions [cf., Anderson, et al. (Ref. 4), and Bier and Hagena (Ref. 5)] have also demonstrated these effects.

A purely mechanical complication is introduced by our use of a movable nozzle at the end of the shock tube. The nozzle (Fig. 1) is machined into a stainless steel sphere which, by a small rotation before and after the test interval, opens and closes the flow passage out of the shock tube. This capability eliminates the need for a secondary diaphragm and reduces the contamination of the vacuum chamber. Although the nozzle is stationary during the actual test interval, timing can be quite critical, and the nozzle position history must be monitored and compared to the test interval for each run. All of the data included in this report were taken in the range of correct nozzle position, although the results of the "off-time" runs can all be explained qualitatively in terms of the measured time variations of various flow properties in the shock tube (see Appendix).

Nozzle Flow Characteristics

Early attempts to detect a molecular beam at the target area were not successful, so we set up our instrumentation in the direct field of flow of the nozzle. A series of tests resolved many problems concerned with timing the shock arrival to coincide with the period in which the nozzle is in the correct position. Heat transfer and ionization-detector records in this field of flow showed a true high-speed flow, and times of flight were measured which correspond to the anticipated thermodynamic limit based on total stagnation enthalpy. The heat transfer measurements were made with thin-film resistance gauges using the analog circuits described by Skinner (Ref. 6). We used a flat-faced cylinder of 1/2 inch diameter.

Mach number effects are not discernable, since the nozzle exit Mach number is already hypersonic. The runs are quite reproducible, and they agree qualitatively with previous measurements for hemisphere-cylinders (Wittliff and Wilson, Ref. 7). The density distribution in the upstream nozzle flow appears to be well correlated by a source flow model with a virtual source near the nozzle exit plane. Further downstream $(x/d > 80)$ the centerline density appears to decrease below that for a source flow. The best fit to the heat transfer measurements is $q/\frac{1}{2}\rho_\infty u_\infty^3 = 0.92\,(Re)^{-.36}$ for Reynolds numbers from 400 to 20,000 based on stagnation viscosity, free stream density, and velocity and probe diameter. We do not yet have sufficient data to completely characterize the flow field, so the above correlation is somewhat tentative, although the data taken at each station with different stagnation densities appear to be very good. We know of no existing theoretical or empirical predictions of hypersonic heat transfer on flat faces, so for the present we must rely on self-consistency to determine the ρ versus x distribution of the flow. The presently indicated pattern is a downstream intersection of the leading characteristics of the expansion waves generated at the nozzle exit. Because this should not occur anywhere near the observed location for an inviscid flow, we attribute the behavior to effects of the nozzle wall boundary layer. The inferred density at $x/d = 120$ is about 45 per cent of that corresponding to the source flow pattern observed upstream.

Further measurements to improve our knowledge of the flow field are planned, but the downstream behavior is of little concern in the configuration we now anticipate using.

Some additional characteristics of the nozzle flow measurements deserve special mention, as they can also affect the later measurements behind skimmers. Aluminum particles torn from the driver-driven diaphragms in previous runs frequently impinge on the gauges during a run. Although over a short period of time these impacts do not cause serious permanent damage to the gauges, they do show up as noise spikes in many of our runs. Over a long period of time they also degrade the gauge quality. The main effect of these particle impacts is to increase the uncertainty in interpretation of data and to increase the number of bad runs. It is mainly because of these particle effects that we have thus far been unable to produce on a single trace an unequivocal quantitative documentation of the skimmer starting effects described in the following, although the accumulated experience of about 130 runs have convinced us they are real. We are currently making several changes in the shock tube system which should drastically reduce the number of particles formed, and instituting a new cleaning procedure which should remove the remainder between runs. The nozzle closes before a significant number of particles from the current run can reach the end of the tube. Canting the beam relative to the nozzle is an effective alternative for solving this problem (Skinner, Ref. 8), but it decreases the margin between the part of the flow used to form the beam and the boundary layer, and would be difficult to incorporate into our present apparatus.

After establishing a satisfactory flow ahead of the skimmer, we made several series of runs with heat transfer gauges and ionization detectors in the post-skimmer flow. During these experiments a heat transfer gauge mounted in the wall of the conical baffle which holds the skimmer was employed as a monitor of the nozzle flow field. This gauge had been previously used in the flow field surveys, so its characteristics were known. The removal of the upstream probe and its replacement by a skimmer did not appear to change the characteristics of this gauge to any measurable degree. This gauge is important to what follows, because it demonstrates that the observed unsteadiness is not due to the upstream flow field, but to a skimmer phenomenon.

In the post-skimmer tests the distance between the nozzle throat and the skimmer was varied from 3 to 15 inches. The heat transfer probe (a flat faced, 1/2-inch cylinder) was located 9-3/8 inches downstream of the skimmer inlet on the flow centerline.

Skimmer Starting

We observed an interesting, reproducible characteristic in the heat transfer records behind skimmers. Figure 2 shows a schematic diagram of this behavior, and an actual record is shown in Fig. 3. We attribute this behavior to a rather novel starting phenomenon in which the flow in the neighborhood of the skimmer develops from an essentially collisionless state to a continuum-like pattern. The latter condition prevails when the local densities are high enough to enforce several collisions of a wall molecule before it can reach the centerline region of the skimmer orifice, thus confining the wall effects to boundary regions near the walls. The short period of high transmission occurs before the cloud of reflected particles can become fully established, resulting in a rapid decay from the initial intensity to a considerably lower value. The time constants for the decay of the initial spike and the buildup of intensity due to the establishment of boundary regions can be characterized in terms of experimentally determined constants by a simple analysis of the integrated incident flux. This starting process seems to be quite distinct from the well-known starting transient normally observed in shock tunnel heat transfer records.

We idealize the behavior in the bottom trace of Fig. 2 by the following sequence of intervals: Region 1) a sharp pulse with an exponential decay caused by an increasing average density in the skimmer entrance and internal passages, Region 2) a rising intensity caused by further increases in density which confine wall molecules to a boundary region of diminishing thickness, and Region 3) a constant intensity region during which the effective boundary region thickness remains constant. This region is often truncated by the end of the test period, before it is completely established.

In Region 1, the average local density due to particles reflected from the skimmer surfaces can be approximated as being proportional to the accumulated incident mass divided by a characteristic volume of the skimmer inlet region:

$$\rho \sim \frac{\rho_\infty u_\infty t}{d} \tag{1}$$

where t is the time measured from the arrival of the pulsed molecular flow at the skimmer station, and d is the diameter of the skimmer entrance. Background gases and "leakage" of reflected gas from the entrance region are ignored.

The average transmitted intensity ratio during this interval can be expressed as $\exp[-K\,\lambda/d]$, where K depends on the skimmer geometry. From Eq. (1) we can express λ as a function of time, to get

$$\left[\frac{I}{I_\infty}\right]_1 = \exp\left[-C_1\,{}^{\lambda_\infty}/u_\infty t\right] \tag{2}$$

As the mass accumulation in the skimmer inlet region proceeds further, the molecules from the skimmer walls become confined to a layer of decreasing thickness. When this thickness (which is some unknown number of λ's) becomes smaller than the inlet radius a core region opens up, and we can characterize the transmitted intensity ratio as

$$\left[\frac{I}{I_\infty}\right]_2 = \left[1-C_2\,{}^{\lambda}/d\right] \tag{3}$$

In the limit of large time a steady flow is established in which λ is constant with time, but for the establishment period (Region 2) we can again use Eq. (1) to get

$$\left[\frac{I}{I_\infty}\right]_2 = \left[1-C_1\,C_2\,\lambda_\infty/u_\infty t\right]^2 \tag{4}$$

We have correlated the measured half-rise times t_1 and t_2 for many shock tube runs at several values of λ_∞/u_∞ in Fig. 3.[2] The uncertainties and scatter are large, but the trends are quite clear. All the data shown are for the skimmer geometry shown in Fig. 4, $d = 0.078$ inch. We base λ on the viscosity of the gas at nozzle stagnation temperature. Back pressure before the run did not have any apparent effect. Most runs were made below 2×10^{-5} torr, but checks at 10^{-4} gave the same results.

Skimmer Transmission Efficiency

Primarily due to the above starting characteristics, we have been unable to get a good measurement of the steady-state transmission ratio except at very high incident intensities. At lower intensities the establishment times are so long that a clear cut measurement is prevented by the short duration of the test flow. At higher intensities we measure a heat transfer ratio of $0.40 \pm .10$. This ratio is the total measured energy flux through the skimmer at the centerline divided by the free stream energy flux measured at the same probe x/d with the skimmer removed. The same value is measured at λ_∞/d of 6.7×10^{-4} and 16.7×10^{-4}. No detectable change in velocity can be found across the skimmer by time of flight measurements, and we attribute the entire attenuation to a loss of mass flux. Calculations indicate that the entire heat transfer gauge is immersed in the post-skimmer flow, but there is no direct method of verifying this assumption with present methods.

CONCLUSIONS AND FUTURE PLANS

The measurements we have described above are in many cases quite crude relative to the ultimate capabilities of the apparatus. We are continually improving our techniques, and many of the quantitative data may change as we eliminate various sources of error. We do feel, however, that enough evidence is available to indicate the best approach for forming a molecular beam of the desired type.

First, it appears that the skimmer starting process plays a crucial role in any high intensity impulse molecular beam. We are now trying different skimmer geometries, as we suspect that the divergence of the internal passages controls transmission at low intensities. We have not yet been able to produce prolonged high transmission at low λ_∞/d (which the primitive ideas given above indicate should be possible) and we feel internal collisions are preventing this (cf., Oman, Ref. 9, Skinner, Ref. 10). Second, it has been shown that a coherent directed flow of high energy can be started almost instantaneously provided the incident flux is high enough. This has been performed without significant loss in energy. Although we have not traversed this flow to prove it is a true molecular beam, it shows the expected expansion rate and does not act like a reexpansion behind the skimmer.

We now intend to base our beam generation on a skimmer operating at high intensity (i.e., close to the nozzle) followed by beam impinging on a collimator which is really a second skimmer operating at a much lower intensity. The evidence we have accumulated thus far indicates that the second skimmer must have a sharply diverging internal passage. This mode of operation is within the capabilities of the present geometric configuration, and is very similar to the configuration presently being employed by Skinner and Fetz (Ref. 11). They have found that the second skimmer only operates well if the first skimmer is also present. The reason for this is not yet understood, but it may be due to the fact that the required internal divergence can only be achieved by large external cone angles. Calculations (Ref. 9) indicate that <u>in a uniform flow field</u> the loss across a low intensity skimmer is a strong function of external angle. The restriction of the incident flow to a beam should greatly reduce this effect.

APPENDIX

SHOCK TUBE UNSTEADINESS EFFECTS

The effects of shock tube wall boundary layers on the steadiness of the reflected-shock fluid state have been well-known for some time. The usual effect is an increase with time of the pressure measured in the end wall stagnation region. This pressure rise originates at the reflected shock, which is encountering an ever-thickening boundary layer and the associated velocity and pressure gradients in the flow generated by the incident shock. The pressure rise is transmitted to the end wall region by compression waves which travel at the local speed of sound. Simple analyses and empirical evidence both indicate a strong, increasing dependence of the rate of pressure rise on incident shock speed, and a decreasing effect of increased Reynolds number based on shock tube diameter.

If we assume the compression waves are isentropic and in equilibrium, the appropriate relations for predicting the effects of these compressions on the density, heat flux,and limiting velocity of the flow can be computed in terms of the ratio of the instantaneous pressure to the pressure measured immediately following reflection. For the present purposes,perfect gas relationships are adequate.

In an isentropic process we can write Gibb's relation as

$$dh = - \frac{1}{\rho}\, dp$$

$$= - RT \frac{dp}{p}$$

Integrating, for a perfect gas, we get

$$h/h_i = \left[\frac{p}{p_i}\right]^{\frac{\gamma-1}{\gamma}} \tag{5}$$

where the subscript i denotes the initial state, in this case that immediately following shock reflection, and γ is the ratio of specific heats for frozen composition.

The free stream energy flux following expansion to maximum velocity can be computed from Eq. (5) and the following

$$\frac{\rho}{\rho_i} = \left[\frac{p}{p_i} \right]^{1/\gamma} \tag{6}$$

$$\frac{u_{max}}{u_{max\ i}} = \left[\frac{h}{h_i} \right]^{1/2} = \left[\frac{p}{p_i} \right]^{\frac{\gamma-1}{2\gamma}} \tag{7}$$

$$\frac{q}{q_i} = \frac{\rho u h}{\rho u h_i} = \left[\frac{p}{p_i} \right]^{\frac{3\gamma-1}{2\gamma}} \tag{8}$$

Equation (8) is applied to the maximum values of p/p_i indicated by the stagnation pressure record from the shock tube, and shows a negligible effect for most of the cases presented. An exception is the "hotter" air run shown on Fig. 3, in which a correction amounting to a factor of 4 has been applied. We feel the application of the maximum correction is justified, as the rise rate is very steep in this case, and the trace levels off at the maximum value for the remainder of the test interval. It is interesting to note that the maximum so achieved is usually quite close to the reflected shock state that would be produced by an ideal shock tube (i.e., no loss in incident shock speed due to boundary layer effects) at the same driver and driven conditions.

REFERENCES

1. Oman, R. A., and Calia, V. S., Interaction of High Energy Gas Molecules with Solid Surfaces, Part II - Progress in an Experimental Investigation of Molecule-Surface Interaction, Grumman Research Department Report RE-166, August 1963 (Final Report on NASr-104).

2. Oman, R. A., Weiser, C. H., and Calia, V. S., Interaction of High Energy Gas Molecules with Solid Surfaces, Grumman Research Department Memorandum RM-215, October, 1962 (Status Report #1 on NASr-104).

3. Brook, J. W., and Oman, R. A., Steady Expansions at High Speed Ratio Using the BGK Kinetic Model, Presented at the Fourth International Symposium on Rarefied Gas Dynamics, Toronto, 1963, to be published as a Grumman Research Department Report.

4. Anderson, J. B., Andres, R. P., Fenn, J. B., and Maise, G., Studies of Low Density Supersonic Jets, Presented at the Fourth International Symposium on Rarefied Gas Dynamics, Toronto, 1964.

5. Bier, K., and Hagena, O., Optimum Conditions for Generating Molecular Beams by Nozzles, Presented at the Fourth International Symposium on Rarefied Gas Dynamics, Toronto, 1964.

6. Skinner, G. T., Analog Network to Convert Surface Temperature to Heat Flux, Cornell Aeronautical Laboratory Report, CAL-100, February 1960.

7. Wittliff, C. E., and Wilson, M. R., Low Density Stagnation Point Heat Transfer in Hypersonic Air Flow, ARL Technical Report 60-333, February 1961.

8. Skinner, G. T., Development of a Shock Tube Driven Molecular Beam, Cornell Aeronautical Laboratory Report RM1396-A-1, October 1961.

9. Oman, R. A., "Analysis of a Skimmer for a High Intensity Molecular Beam Using a Three Fluid Model," The Physics of Fluids, Vol. 6, July 1963.

10. Skinner, G. T., "Molecular Beam for the Study of High Temperature Gas Collision Processes," The Physics of Fluids, Vol. 4, pp. 1172-1176, September 1961.

11. Skinner, G. T., and Fetz, B. H., Measurement of Normal Momentum Accommodation Coefficients with a 1.2 EV Pulsed Beam, Presented at the Fourth International Symposium on Rarefied Gas Dynamics, Toronto, 1964.

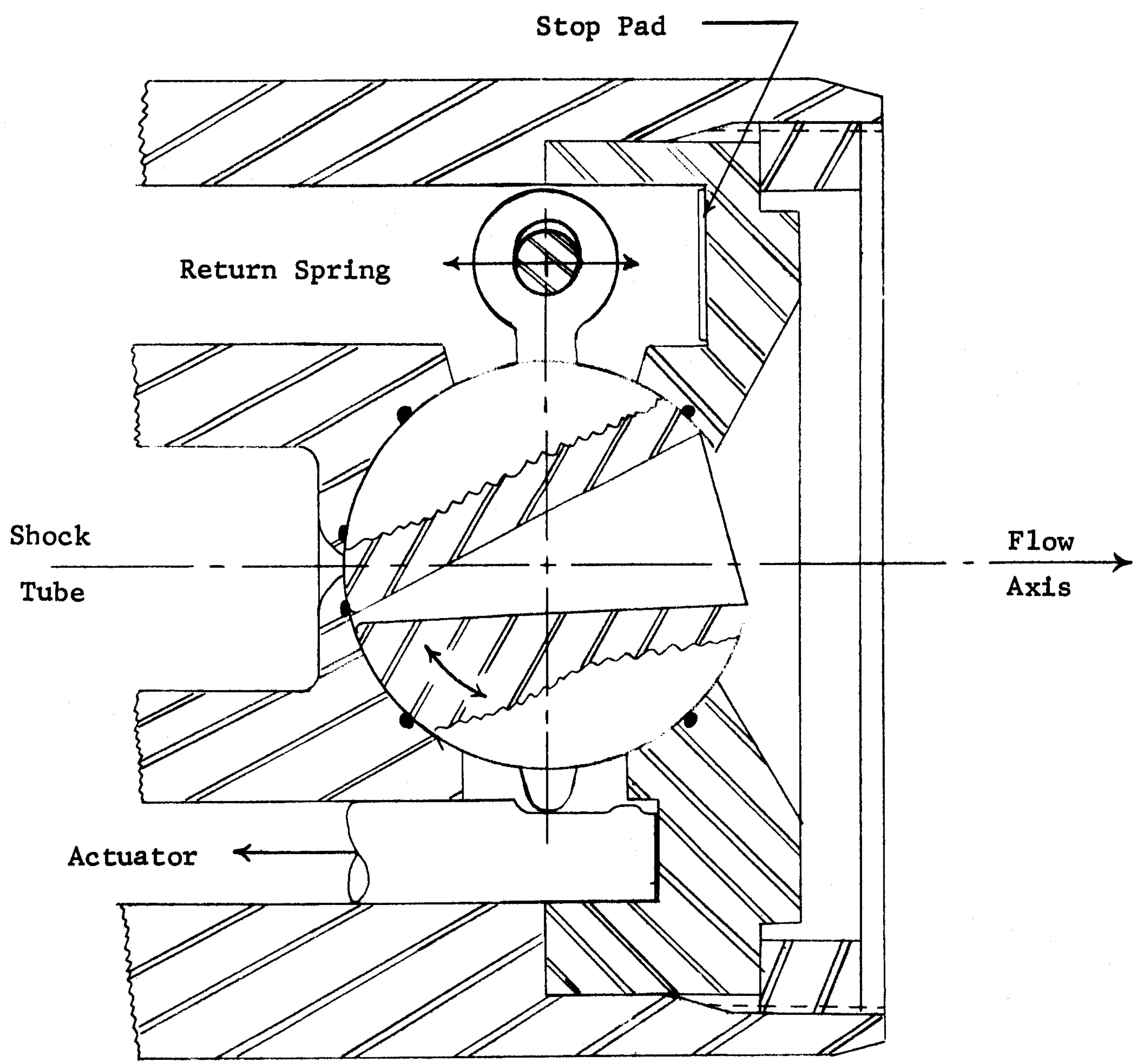

Fig. 1 Nozzle Mechanism in Initial Position

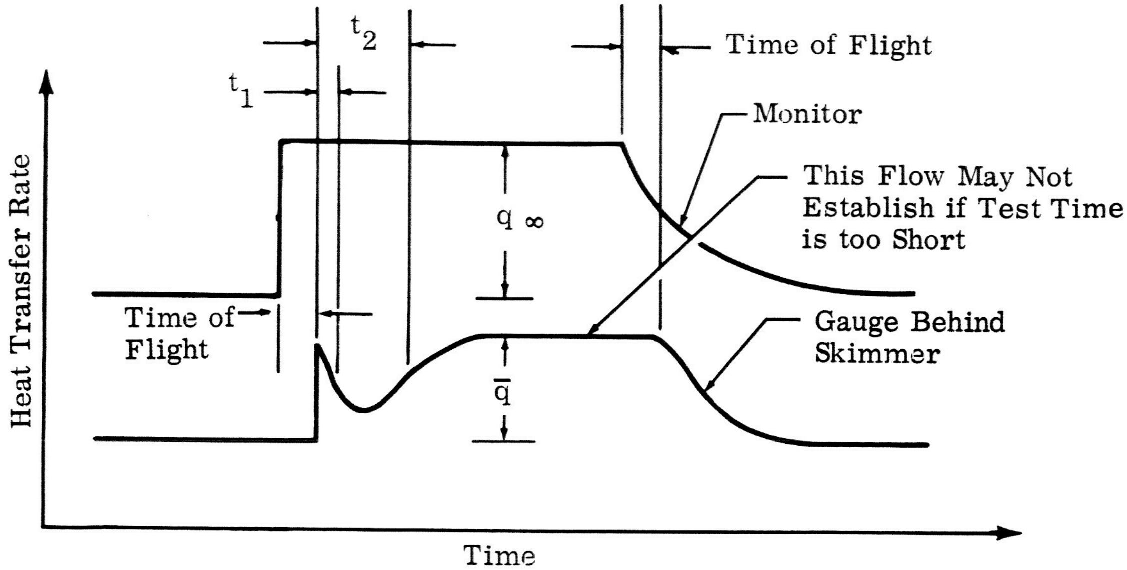

Fig. 2 Idealized Pattern of Heat Transfer Behind Skimmer

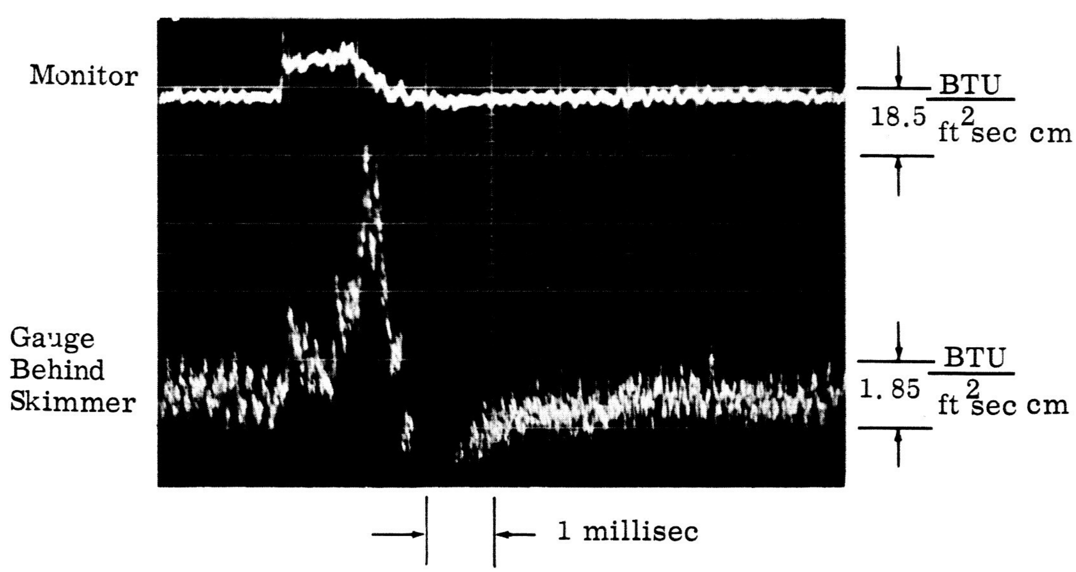

Fig. 3 Observed Pattern of Heat Transfer Behind Skimmer

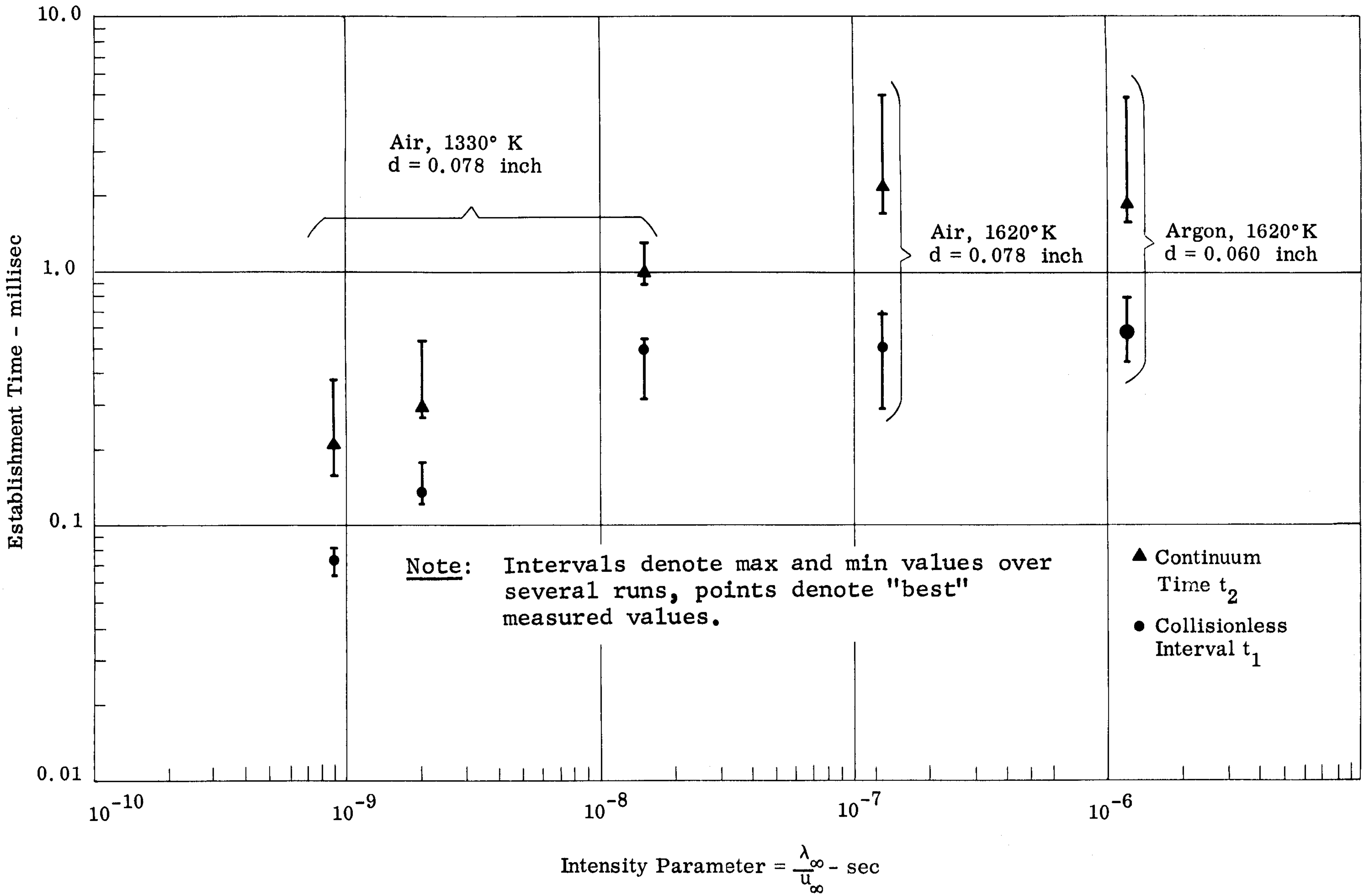

Fig. 4 Continuum and Collisionless Intervals Measured for Skimmer Starting Process

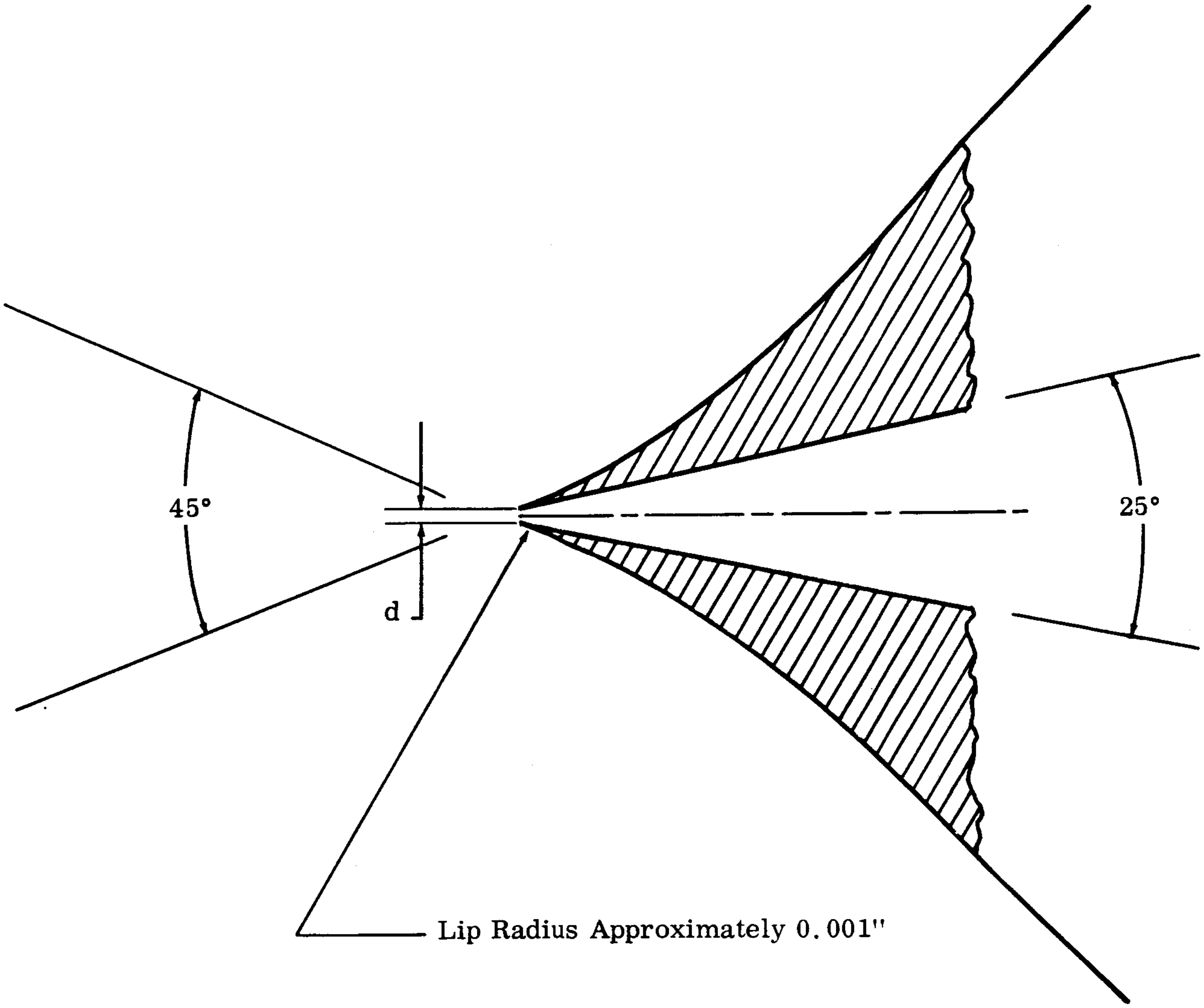

Fig. 5 Present Skimmer Geometry